Glial molecular alterations with mouse brain development and aging: up-regulation of the Kir4.1 and aquaporin-4

Rajaneesh Kumar Gupta · Madhusudan Kanungo

Abstract Glial cells, besides participating as passive supporting matrix, are also proposed to be involved in the optimization of the interstitial space for synaptic transmission by tight control of ionic and water homeostasis. In adult mouse brain, inwardly rectifying K+ (Kir4.1) and aquaporin-4 (AQP4) channels localize to astroglial endfeets in contact with brain microvessels and glutamate synapses, optimizing clearance of extracellular K^+ and water from the synaptic layers. However, it is still unclear whether there is an age-dependent difference in the expressions of Kir4.1 and AQP4 channels specifically during postnatal development and aging when various marked changes occur in brain and if these changes region specific. RT-PCR and immunoblotting was conducted to compare the relative expression of Kir4.1 and AQP4 mRNA and protein in the early and mature postnatal (0-, 15-, 45-day), adult (20-week), and old age (70-week) mice cerebral and cerebellar cortices. Expressions of Kir4.1 and AQP4 mRNA and protein are very low at 0-day. A pronounced and continuous increase was observed by mature postnatal ages (15-, 45-days). However, in the 70-week-old mice, expressions are significantly up-regulated as compared to 20-week-old mice. Both genes follow the same age-related pattern in both cerebral and cerebellar cortices. The time course and expression pattern suggests that Kir4.1 and AQP4 channels may play an important role in brain K^+ and water homeostasis in early postnatal weeks after birth and during aging.

Keywords Kir4.1 · AQP4 · Glia · Postnatal development · Aging · K+ and water homeostasis

R. K. Gupta (✉) · M. Kanungo
Molecular Biology & Biochemistry Lab., Centre of Advance Study in Zoology, Banaras Hindu University, Varanasi 221005 Uttar Pradesh, India
e-mail: guptarajaneesh@gmail.com

Introduction

Glial cells undergo several changes after birth and during aging at the functional and molecular level (Freeman 2010; Modi and Kanungo 2010; Rice and Barone 2000; Kanungo 1994). K^+ and water homeostasis is one of the important phenomenons in the brain that is primarily controlled by astrocytes (Simard and Nedergaard 2004). Extracellular K^+ efflux from active neurons is passively taken up by astrocytes via strongly rectifying heteromeric Kir4.1/Kir5.1 and Kir4.1/2.1 channels, redistributed throughout the astrocytic syncytium via gap junctions and is then extruded from glia into extracellular "sinks" (blood vessels, cerebrospinal fluid (CSF) or other region of low K^+ concentration) via weakly rectifying Kir4.1 homomeric channels (Butt and Kalsi 2006). This glial K^+ spatial buffering prevents K^+ build-up in the narrow brain extracellular space, which would affect transmitter release (Erulkar and Weight 1977; Gage and Quastel 1965) and electrical properties of axons (Malenka et al. 1981). Water flux via AQP4 water channel is linked to K^+ spatial buffering (Niermann et al. 2001; Holthoff and Witte 1996). This association between K^+ and osmotic homeostasis is supported by

the structural evidence; colocalization of Kir4.1 and AQP4 in glial membranes (Nagelhus et al. 2004; Takumi et al. 1998), and functional evidences; AQP4 gene deletion in mice reduces seizure susceptibility and increases seizure duration (Binder et al. 2006, 2004), greatly reduces auditory evoked potentials responses (Li and Verkman 2001), and mildly reduces electroretinogram potentials (Li et al. 2002). Moreover, cellular K^+ reuptake from brain extracellular space is impaired in AQP4 null mice in models of neuroexcitation, including cortical spreading depression (Padmawar et al. 2005) and electrical seizure induction (Binder et al. 2006). A similar seizure phenotype and delay in K^+ uptake was found in α-syntrophin knockout mice that manifest altered glial cells AQP4 localization (Neeley et al. 2001). Further, several studies also indicate that K^+ and osmotic fluxes are coupled in glia-swelling conditions (Dibaj et al. 2007; Pannicke et al. 2004).

During early postnatal development of brain, the extracellular space makes up a large fraction of the brain volume (volume fraction 0.36) and allows ready diffusion of K^+ and water. However, as neural cells proliferate and grow, the extracellular space gradually diminishes and reaches the volume fraction 0.2 in adult brain (Lehmenkühler et al. 1993). In aged brain, it further reduces to attain its minimum volume fraction in life span (0.18) (Sykova et al. 1998). This decrease in extracellular space after birth cannot accommodate the neuronal activity-generated ion and water fluxes (Gardner-Medwin 1983). Therefore, it is necessary that neural cells engender mechanisms for K^+ and osmotic homeostasis that can compensate for the loss of a large extracellular distribution volume. A failure to maintain the ion and osmotic fluxes at the site of high neuronal activity would tend to cause neuronal depolarization, hyperexcitability, and seizures. Since seizures are particularly common in newborns (Lombroso 1996), it is of importance to unveil how these homeostatic mechanisms develop. On the other end, during aging, the movement of ions and neurotransmitters are more hindered due to smaller extracellular space (ECS) (Sykova et al. 1998) that consummate in greater susceptibility of the aging brain to anoxia/ischemia, apparently due to a faster extracellular acidosis and accumulation of K^+. It is still unclear as to how the brain adapts homeostatic mechanisms to maintain the ion and water homeostasis in aging brain. We hypothesized that Kir4.1 and AQP4 in mice brain are very essential for K^+ and water handling after birth and during aging as well. Therefore, we performed this study to elucidate the age-dependent profile of Kir4.1 and AQP4 in the mouse cerebral and cerebellar cortices using RT-PCR and immunoblotting. We chose cortical regions (cerebral and cerebellar) of brain in which the adult pattern of expression and cellular/sub-cellular localization has been widely studied in detail (Butt and Kalsi 2006; Venero et al. 2001).

Materials and methods

Animals

Male AKR strain mice were used for the experiments. The maximum life span of these mice under in our laboratory conditions is 75 ± 5 weeks. They were maintained at 12 h light and dark schedule with ad libitum standard mice feed and drinking water in an animal house at ambient temperature. The procedure for use and handling of animals were in accordance with the guidelines approved by the Institutional Animal Ethical Committee of Banaras Hindu University. 0-day mice were decapitated for excising the brain. The mice of other ages were sacrificed by cervical dislocation. After sacrifice, whole cerebral and cerebellar cortices were peeled off by surgical fine forceps under dissecting microscope. Meninges and white matter were removed from cortices carefully as much as possible. One half of each was processed for RT-PCR and the other cortical half for immunoblotting.

Chemicals

Analytical grade chemicals were used for all the experiments. Molecular biology grade chemicals were used wherever necessary. All the chemicals and enzymes were used as per manufacturer's instructions.

Experimental design

RNA extraction

RNA extraction from mice brain of all ages was performed using the TRI reagent (Sigma-Aldrich)

according to the manufacturer's directions and was dissolved in diethylpyrocarbonate (DEPC)-treated water. RNA was stored at −80°C until use.

DNase-I digestion and RNA quantification

Extracted RNA was treated with DNase-I (DNA-free™, Ambion) according to the manufacturer's guidelines to remove any DNA contamination. RNA concentration was calculated by measuring the absorbance by a UV–vis spectrophotometer at 260 nm after appropriate dilution. The integrity of the RNA samples was verified by 1% formaldehyde agarose gel electrophoresis containing 20 mM MOPS, 8 mM Na-acetate, 1 mM EDTA, and 2.2 M formaldehyde.

Reverse transcription

To synthesize the first strand of cDNA, 2 μg of total RNA and 200 ng random hexamer primer (MBI Fermentas) were mixed, and reaction volume was made up to 11 μl. It was incubated at 70°C for 5 min and chilled on ice. After that, 2 μl of 5× reaction buffer, 2 μl of 10 mM dNTP mix and 20 U of RNase inhibitor (Ribolock™, MBI Fermentas) were added, and the volume was made up to 19 μl. The tube was incubated for 5 min at 25°C, and 200 U of M-MuLv reverse transcriptase (New England Biolabs) was added. Further, the tube was incubated for 10 min at 25°C and then at 42°C for 1 h in thermal cycler (Mini cycler™, MJ Research). The reaction was terminated by heating at 70°C for 10 min, and after chilling on ice, the tube was stored at −80°C or directly used for the PCR reaction.

Polymerase chain reaction

Expression of Kir4.1, AQP4, and β-actin was assessed by polymerase chain reaction (PCR) using the following gene-specific primers: 5′ TACAGTCAGACGACTCAGACA 3′ and 5′ GAAGCAGTTTGCCTGTCACCT 3′ for Kir4.1; 5′ GGAAGGCTAGGTTGGTGACTTC 3′ and 5′ TGGTGACTCCCAATCCTCCAAC 3′ for AQP4; 5′ ATCGTGGGCCGCTCTAGGCACC 3′ and 5′ CTCTTTGATGTCACGCACGATTTC 3′ for β-actin. The annealing temperature and the primers' amount was validated for proper amplification of each amplicon. The co-amplification was carried out in a 25-μl reaction mixture containing 2 μl of cDNA, 2.5 μl of 10× Taq polymerase buffer with 15 mM MgCl$_2$, 0.6 mM of each dNTP, 3 U of Taq polymerase (Bangalore genei), and 10 pmol of forward and reverse primers. The samples were denatured at 94°C for 5 min and amplified using the following amplification parameters: denaturation at 94°C for 1 min, primer annealing at 57°C (for Kir4.1) or 60°C (for AQP4) for 1 min, elongation at 72°C for 1 min. The number of cycles used for co-amplification was chosen to be within the exponential phases of co-amplification of all amplicons. Polyacrylamide gel (6%) was used to resolve the amplified products. Subsequently, ethidium bromide staining was performed.

Tissue lysate preparation

Cerebral and cerebellar cortices of different ages were homogenized in 50 mM Tris–Cl, (pH 7.4), containing 0.2% triton X-100, 5 mM ethylenediaminetetraacetic acid, 5 mM ethylene glycol tetraacetic acid, 2 mM phenylmethanesulfonylfluoride, 5 mM benzamidine, 2 mM mercaptoethanol (β-ME), and protease inhibitor cocktail (Sigma-Aldrich). Protein was estimated by Bradford method using BSA as standard (Bradford 1976).

SDS-polyacrylamide gel electrophoresis

For immunoblotting, 25 μg of crude sample was denatured in Laemelli gel loading buffer (100 mM Tris–Cl (pH 6.8), 2% sodium dodecyl sulfate (SDS), 2% β-ME, 20% glycerol, and 0.2% bromophenol blue) in boiling water bath for 5 min. The samples were loaded on 10% SDS-polyacrylamide gel along with prestained protein marker (MBI Fermentas). Electrophoresis was carried out in gel running buffer containing 250 mM glycine, 25 mM Tris, and 0.1% SDS. For proper stacking, the samples were run at 15 mA in stacking gel and resolved at 30 mA in resolving gel.

Immunoblotting and detection

After electrophoresis, proteins were transferred onto the PVDF membrane (Millopore) overnight at 4°C with constant power supply of 50 V. After transfer, the membrane was blocked in 5% nonfat milk in phosphate buffered saline (PBS) (pH 7.4) for 4 h at room temperature. The blot was then incubated with mouse monoclonal anti-Kir4.1 (1: 2,000 dilution,

Sigma Aldrich) or rabbit polyclonal anti- AQP4 (1:1,000 dilution, Santa Cruz) or rabbit monoclonal anti-β-actin (1:20,000, Sigma-Aldrich) in 5% nonfat milk and 0.05% Tween- 20 in PBS (pH 7.4) overnight at 4°C. After three washes with PBST (PBS+0.05% Tween-20) for 5 min each, the blot was incubated with HRP-conjugated goat anti-mouse (1:5,000) or goat anti-rabbit IgG (1:10,000 dilution, Bangalore Genei) in PBS (pH 7.4) containing 5% nonfat milk and 0.05% Tween 20 for 4 h at room temperature. After washing with PBST (pH 7.4), immunoreactive proteins were revealed with ECL super signal west pico kit (Pierce Biotechnology) in X-ray film, and their expression level was measured by densitometry. β-actin was used as control for immunoblotting. Band density values were normalized to β-actin.

Data and statistical analysis

All the experiments were repeated three times ($n=5$/age). The gels and X-ray film exposures were photographed by a digital camera (Nikon Corporation, Japan). The bands were analyzed, and quantitation was done using computer-assisted densitometry (AlphaEase FCTM software, Alpha Innotech Corporation, CA). For RT-PCR, the signal intensity of the target band, and for immunoblots, monomeric as well as higher oligomeric bands were measured after normalization with β-actin and expressed as relative densitometric value (RDV). Results represent the mean±SEM of data obtained from three different sets of experiments. The mean±SEM was analyzed by Sigma Stat 2.0 software. All the data were examined by one-way ANOVA followed by Student–Newman–Keuls test. $P<0.05$ was taken as statistically significant (95% confidence interval).

Results

Optimization of number of cycle for PCR co-amplification

RT-PCR was optimized to co-amplify Kir4.1+β-actin as 634 and 543 bp; AQP4+β-actin as 460 and 543 bp fragments of respective cDNAs. Simultaneous amplification of β-actin gene as an internal control added the advantage to compensate for the intra- and inter-assay variability during reverse transcription and PCR

reactions. We checked the non-interference of Kir4.1 and AQP4 primers with β-actin primers used to detect different targets in a single PCR reaction (data not shown). Further, to quantify genes expression, the number of PCR cycles was optimized to be fall into the exponential phases of the co-amplification reactions for both amplicons. PCR co-amplification was performed for 26–36 cycles and 24–34 for Kir4.1+β-actin and AQP4+β-actin respectively. To achieve the overlapping exponential phase for Kir4.1 or AQP4 with β-actin amplicon, β-actin primers were added after ten cycles of Kir4.1 or AQP4 amplification. The number of cycles optimized for Kir4.1 and AQP4 was 30 and 32, respectively, to achieve amplification in linear range (Fig. 1a, b).

Semi-quantitative RT-PCR of Kir4.1

Semi-quantitative RT-PCR of Kir4.1 of cerebral cortex (Fig. 2a) shows that Kir4.1 was expressed at very low levels at 0 day compared with the levels at 45 days ($P<0.05$). A significant increase in Kir4.1 level is noted from 0 to 15 days ($P<0.05$). Further, its expression is significantly highest in 45 days ($P<0.05$) as compared to that of other ages. However, its expression is up-regulated in 70 days in comparison to 20-day-old mice ($P<0.05$).

For cerebellar cortex (Fig. 2b), expression of Kir4.1 gene is significantly low at 0 day ($P<0.05$). Its highest expression is found at 45 days ($P<0.05$). Its expression is significantly higher in 70-week-old mice as compared to that of 20-week-old mice ($P<0.05$).

Semi-quantitative RT-PCR of AQP4

RT-PCR of AQP4 gene of cerebral cortex (Fig. 3a) shows that its expression is lowest at 0 day compared with the levels at 45 days ($P<0.05$). A significant increase in AQP4 level was noted from 0 to 15 days ($P<0.05$). Further, its expression is significantly highest in 45 days ($P<0.05$) as compared to that of other ages. However, its expression is up-regulated in 70 days in comparison to 20-day-old mice ($P<0.05$).

For cerebellar cortex (Fig. 3b), expression of AQP4 gene is significantly low at 0 day ($P<0.05$). Its highest expression is found at 45 days ($P<0.05$). Its expression is significantly higher in 70-week-old mice as compared to that of 20-week-old mice ($P<0.05$).
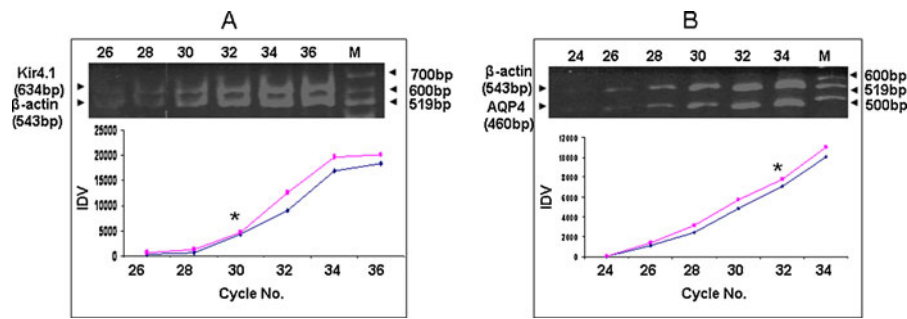
Fig. 1 Determination of linearity of PCR coamplifications. Integrated density value (IDV) of the PCR products obtained by different number of cycles is presented as a function of PCR cycle numbers. Optimal linear range is shown by *asterisk*. **a** PCR product of 634 and 543 bp for Kir4.1 and β-actin mRNA, respectively. *M* denotes marker 100 bp DNA ladder **b** PCR product of 460 and 543 bp for AQP4 and β-actin mRNA, respectively

Immunoblot analysis of Kir4.1

To detect Kir4.1 protein, a rabbit polyclonal antibody specific to Kir4.1 peptide was used. It detects Kir4.1 monomer as ~38 kDa. Its expression in the cerebral cortex (Fig. 4a) increases significantly from 0 till 45 days ($P<0.05$). Its highest expression is seen at 45 days ($P<0.05$). In newborn mice, its expression is significantly low ($P<0.05$) as compared to 45 days. However, its expression is significantly up-regulated in 70-day mice as compared to that of 20-day mice ($P<0.05$). In the cerebellar cortex, Kir4.1 (Fig. 4b) expression is very low at 0 day ($P<0.05$). Its expression increases significantly till 45 days ($P<0.05$), and its expression is significantly up-regulated in 70-day mice as compared to that of 20-day mice ($P<0.05$).

Immunoblot analysis of AQP4

To detect AQP4 protein, a rabbit polyclonal antibody specific to AQP4 peptide was used. It detects AQP4 as ~32 kDa. Its expression in the cerebral cortex (Fig. 5a) increases significantly from 0 till 45 days ($P<0.05$). Its highest expression is seen at 45 days ($P<0.05$). In newborn mice, its expression is significantly low ($P<0.05$) as compared to 45 days. However, its expression is significantly up-regulated in 70-day mice as compared to that of 20-day mice ($P<0.05$). In the cerebellar cortex, AQP4 (Fig. 5b) expression is very low at 0 day ($P<0.05$). Its expression increases significantly till 45 days ($P<0.05$), and its expression is significantly up-regulated in 70-day mice as compared to that of 20-day mice ($P<0.05$).
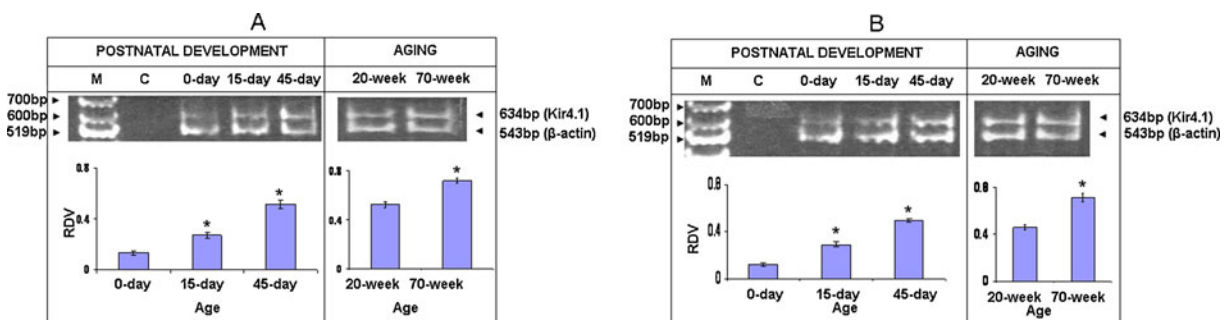

Fig. 2 RT-PCR of Kir4.1 gene of cerebral cortex (**a**) and of cerebellar cortex (**b**) of mice of postnatal and old ages. *M* denotes marker 100 bp DNA ladder. *C* denotes negative control. Histograms represent cumulative data expressed as mean±SEM obtained from three different sets of experiments conducted for cerebral cortex and cerebellar cortex, respectively. *Significant from previous age group; $P<0.05$. RDV denotes relative densitometric value
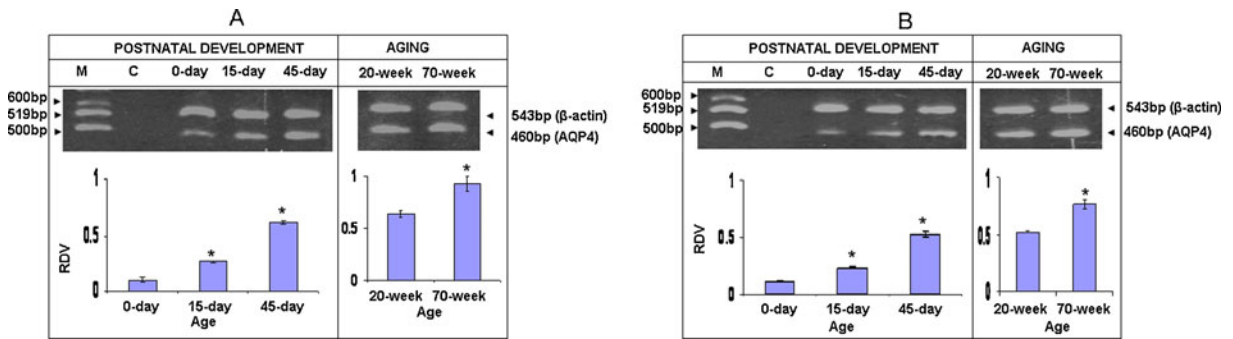
Fig. 3 RT-PCR of AQP4 gene of cerebral cortex (a) and of cerebellar cortex (b) of mice of postnatal and old ages. *M* denotes marker 100 bp DNA ladder. *C* denotes negative control. Histograms represent cumulative data expressed as mean±SEM obtained from three different sets of experiments conducted for cerebral cortex and cerebellar cortex, respectively. *Significant from previous age group; $P<0.05$

Discussion

Glia are the major brain cellular compartment that changes with age; they may thus contribute significantly to the maintenance of brain integrative ability and adaptation with age. Brain K^+ and water transport is poorly understood at the molecular level, and marked changes occur during brain development and aging. As the glial genes—Kir4.1 and AQP4, regulate K^+ and water homeostasis in brain, the expression levels of Kir4.1 and AQP4 gene in the cerebral and cerebellar cortices was studied as a function of age to find out when their expression start, peak, and decline. The present study also throws light on the relative expression level of Kir4.1 and AQP4 in cerebral and cerebellar cortices.

RT-PCR and immunoblot analysis of Kir4.1 and AQP4 in cerebral and cerebellar cortices show that their expressions start from 0 day at both RNA and protein levels. During development, their expressions increase till 45 days. Our result supports the previous study of Wen et al. (1999) and a recent study of Hsu et al. (2011). After birth glial cells start express Kir4.1 and AQP4 at a time when the volume fraction of the ECS declines progressively. It is noteworthy that evoked neuronal activity in rodent cortical slices causes a pronounced shrinkage of the extracellular space at 2–3 weeks of age (Ransom et al. 1985). Therefore, a failure to develop and maintain a mechanism to accommodate K^+ ion and water fluxes that are generated by neural activity may leads to neuronal depolarization and excessive discharge in early
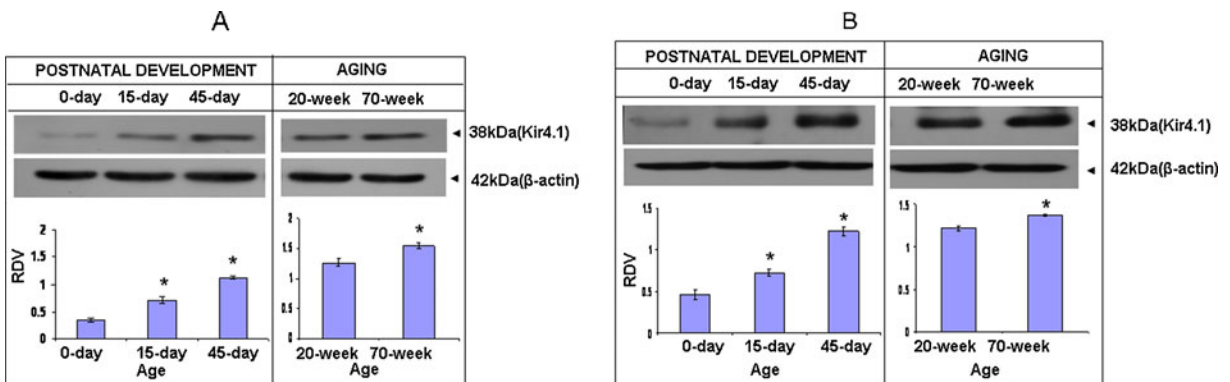

Fig. 4 Immunoblot showing ~38 kDa band of Kir4.1 monomeric protein of cerebral cortex (a) and of cerebellar cortex (b) of mice of postnatal and old ages. Histogram represent cumulative data expressed as mean±SEM obtained from three different sets of experiments conducted for cerebral cortex and cerebellar cortex, respectively. *Significant from previous age group; $P<0.05$
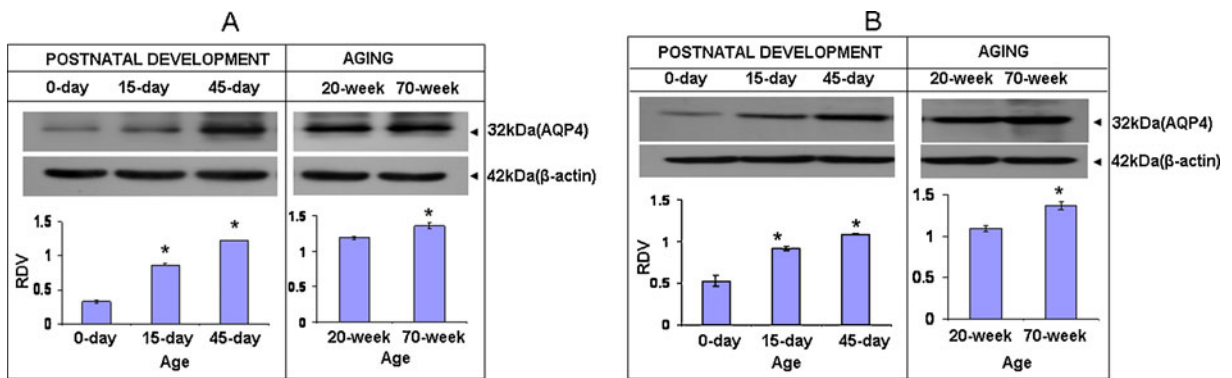
Fig. 5 Immunoblot showing ~32 kDa band of AQP4 monomeric protein of cerebral cortex (a) and of cerebellar cortex (b) of mice of postnatal and old ages. Histogram represent cumulative data expressed as mean±SEM obtained from three different sets of experiments conducted for cerebral cortex and cerebellar cortex, respectively. *Significant from previous age group; $P<0.05$

postnatal ages. However, the regulatory mechanisms for K^+ and coupled water fluxes in the shrinked ECS are still far from clear. An activity-dependent shrinkage of the ECS is considered to reflect glial K^+ buffering and its obligatory coupling to osmotic uptake (Dietzel et al. 1980). During postnatal development, the expression of Kir4.1 and AQP4 may be functionally inter-reliant. The up-regulation in the expression of Kir4.1 and AQP4 after birth may be concomitant with the development of extracellular K+ buffering capacity during the first 2–3 weeks (Connors et al. 1982). Further, since several studies have shown that these channel proteins regulate glial proliferation, differentiation, and migration (Kong et al. 2008; Yasuda et al. 2008), it is worth to hypothesize that both proteins may possibly involve to regulate brain growth during normal postnatal development which appears to be due, in different periods, to different combinations of increased or decreased numbers of neurons, increased numbers of glial cells, or modification of neuronal and glial cell sizes.

Our results, interestingly, show that the expression of Kir4.1 and AQP4 are significantly up-regulated in old mice as compared to that of adult mice. It has been shown that there is an increase in the vulnerability of astrocytes to oxidative damage with age (Papadopaulos et al. 1997). Early onset of a sudden and profound depolarization of neurons and glia during anoxia, and a diminished subsequent recovery of synaptic activity also suggest for increased vulnerability in aging rodents (Roberts et al. 1990; Roberts

and Chih 1995). Further, recent study also indicates that aged rats are vulnerable to seizures induced by dyshomeostasis of potassium and chloride ions in the hippocampal extracellular fluid (Takeda et al. 2008). In old age, since size and tortuosity of ECS around neurons are significantly lowered (Sykova et al. 1998). Thus, it may slow down the diffusion of neuroactive substances like ions and glutamate between distinct synapses (Barbour and Hausser 1997; Kullmann and Asztely 1998). The age-related enhancement in the levels of Kir4.1 and AQP4 may contribute to maintain K^+ and water homeostasis between the synapses to cope up with the increased burden of ion and neurotransmitters in narrower ECS.

Further, aged brains often display a decrease in the number of neurons and a relative increase in glial elements (Henderson et al. 1980; Scheibel and Scheibel 1975). Hayakawa et al. (2007) reported that the number of astrocytes increases in hippocampus during aging. Astrocytes proliferate and activate in the hippocampus with advancing age (Hayakawa et al. 2007). Our data shows that advancing age is associated with increased expression of Kir4.1 and AQP4 mRNA and protein. This increase may reflect a potentially beneficial response to the wear and tear of aging, as Kir4.1 is known to promote spatial K^+ buffering (Butt and Kalsi 2006), oligodendrocyte development, and in vivo myelination (Neusch et al. 2001). It has also been shown that gain of function of Kir4.1 channel increases cell resistance to changes of potassium fluxes and cell volume evoked by ammonia and hypoosmotic stress (Michlewska et al. 2010).

Further, AQP4 plays a crucial role in regulating the proliferation, migration, and differentiation of adult neural stem cells, and this function of AQP4 is probably mediated by its action on intracellular Ca2+ dynamics (Kong et al. 2008). In the light of the known action of Kir4.1 and AQP4, together as well as separately, these results indicate that (a) increased expression of Kir4.1 and AQP4 during development is important for brain development and establishment of ion and water homeostasis and may be relevant for the understanding of how regulation of brain K^+ and water homeostasis is enhanced postnatally; (b) increased Kir4.1 and AQP4 expressions are an important response to age-related changes in the brain; (c) age-related overexpression of Kir4.1 an AQP4 contributed to adaptive response of the glial cells in old age to maintain K^+ and water homeostasis.

References

Barbour B, Hausser M (1997) Intersynaptic diffusion of neurotransmitter. Trends Neurosci 20:377–384

Binder DK, Oshio K, Ma T, Verkman AS (2004) Increased seizure threshold in mice lacking aquaporin-4 water channels. Neuroreport 15:259–262

Binder DK, Yao X, Zador Z, Sick TJ, Verkman AS, Manley GT (2006) Increased seizure duration and slowed potassium kinetics in mice lacking aquaporin-4 water channels. Glia 53:631–636

Bradford MM (1976) A rapid and sensitive method for the quantitation of microgram quantities of protein utilizing the principle of protein-dye binding. Anal Biochem 72:248–254

Butt AM, Kalsi A (2006) Inwardly rectifying potassium channels (Kir) in central nervous system glia: a special role for Kir4.1 in glial functions. J Cell Mol Med 10:33–44

Connors BW, Ransom BR, Kunis DM, Gutnick MJ (1982) Activity-dependent K^+ accumulation in the developing rat optic nerve. Science 216:1341–1343

Dibaj P, Kaiser M, Hirrlinger J, Kirchhoff F, Neusch C (2007) Kir4.1 channels regulate swelling of astroglial processes in experimental spinal cord edema. J Neurochem 103:2620–2628

Dietzel I, Heinemann U, Hofmeier G, Lux HD (1980) Transient changes in the size of the extracellular space in the sensorymotor cortex of the cats in relation to stimulus-induced changes in the potassium concentration. Exp Brain Res 40:432–439

Erulkar SD, Weight FF (1977) Extracellular potassium and transmitter release at the giant synapse of the squid. J Physiol 226:209–218

Freeman MR (2010) Specification and morphogenesis of astrocytes. Science 330:774–778

Gage PW, Quastel DMJ (1965) Dual effect of potassium on transmitter release. Nature 206:625–626

Gardner-Medwin AR (1983) A study of the mechanisms by which potassium moves through brain tissue in the rat. J Physiol 335:353–374

Hayakawa N, Kato H, Araki T (2007) Age-related changes of astrocytes, oligodendrocytes and microglia in the mouse hippocampal CA1 sector. Mech Ageing Dev 128:311–316

Henderson G, Tomlinson BE, Gibson PH (1980) Cell counts in human cerebral cortex in normal adults throughout life using an image analyzing computer. J Neurol Sci 46:113–136

Holthoff K, Witte OW (1996) Intrinsic optical signals in rat neocortical slices measured with near-infrared dark-field microscopy reveal changes in extracellular space. J Neurosci 16:2740–2749

Hsu MS, Seldin M, Lee DJ, Seifert G, Steinhäuser BDK (2011) Laminar-specific and developmental expression of aquaporin-4 in the mouse hippocampus. Neuroscience 178:21–32

Kanungo MS (1994) Genes and aging. Cambridge University Press, Cambridge/New York, pp 167–245

Kong H, Fan Y, Xie J, Ding J, Sha L, Shi X, Sun X, Hu G (2008) AQP4 knockout impairs proliferation, migration and neuronal differentiation of adult neural stem cells. J Cell Sci 121:4029–4036

Kullmann DM, Asztely F (1998) Extrasynaptic glutamate spillover in the hippocampus: evidence and implications. Trends Neurosci 21:8–14

Lehmenkühler A, Sykova E, Svoboda J, Zilles K, Nicholson C (1993) Extracellular space parameters in the rat neocortex and subcortical white matter during postnatal development determined by diffusion analysis. Neuroscience 55:339–351

Li J, Verkman AS (2001) Impaired hearing in mice lacking aquaporin-4 water channels. J Biol Chem 276:31233–31237

Li J, Patil RV, Verkman AS (2002) Mildly abnormal retinal function in transgenic mice without müllar cell aquaporin-4 water channels. Invest Ophthalmol Vis Sci 43:573–579

Lombroso CT (1996) Neonatal seizures: a clinician's overview. Brain Dev 18:1–28

Malenka RC, Kocsis JD, Ransom BR, Waxman SG (1981) Modulation of parallel fiber excitability by postsynaptically mediated changes in extracellular potassium. Science 214:339–341

Michlewska MO, Jiang H, Aschner M, Albrecht J (2010) Gain of function of Kir4.1 channel increases cell resistance to changes of potassium fluxes and cell volume evoked by ammonia and hypoosmotic stress. Pharmacol Rep 62:1237–1242

Modi PK, Kanungo MS (2010) Age-dependent expression of S100β in the brain of mice. Cell Mol Neurobiol 30:709–716

Nagelhus EA, Mathiisen TM, Ottersen OP (2004) Aquaporin-4 in the central nervous system: cellular and subcellular

distribution and coexpression with KIR4.1. Neuroscience 129:905–913

Neeley JD, Amiry-Moghaddam M, Ottersen OP, Froehner SC, Agre P, Adams ME (2001) Syntrophin-dependent expression and localization of aquaporin-4 water channel protein. Proc Natl Acad Sci USA 98:14108–14113

Neusch C, Rozengurt N, Jacobs RE, Lester HA, Kofuji P (2001) Kir4.1 potassium channel subunit is crucial for oligodendrocyte development and in vivo myelination. J Neurosci 21:5429–5438

Niermann H, Amiry-Moghaddam M, Holthoff K, Witte OW, Ottersen OP (2001) A novel role of vasopressin in the brain: modulation of activity-dependent water flux in the neocortex. J Neurosci 21:3045–3051

Padmawar P, Yao X, Bloch O, Manley GT, Verkman AS (2005) K^+ waves in brain cortex visualized using a long-wavelength K^+-sensing fluorescent indicator. Nat Methods 2:825–827

Pannicke T, Iandiev I, Uckermann O, Biedermann B, Kutzera F, Wiedemann P, Wolburg H, Reichenbach A, Bringmann A (2004) A potassium channel-linked mechanism of glial cell swelling in the postischemic retina. Mol Cell Neurosci 26:493–502

Papadopoulos MC, Koumenis IL, Yuan TY, Giffard RG (1997) Increased vulnerability of astrocytes to oxidative injury with age despite constant antioxidant defenses. Neuroscience 82:915–925

Ransom BR, Yamate CL, Connors BW (1985) Activity-dependent shrinkage of extracellular space in rat optic nerve: a developmental study. J Neurosci 5:525–532

Rice D, Barone SJ (2000) Critical periods of vulnerability for the developing nervous system: evidence from humans and animal models. Environ Heal Perspect 108:511–533

Roberts EL, Chih CP (1995) Age-related alterations in energy metabolism contribute to the increased vulnerability of the aging brain to anoxic damage. Brain Res 678:83–90

Roberts EL, Rosenthal M, Slick TJ (1990) Age-related modifications of potassium homeostasis and synaptic transmission during and after anoxia in rat hippocampal slices. Brain Res 514:111–118

Scheibel ME, Scheibel AB (1975) Structural changes in the aging brain. In: Brody H, Herman D, Ordy JM (eds) Aging, vol. 1. Raven Press, New York, pp 11–37

Simard M, Nedergaard M (2004) The neurobiology of glia in the context of water and ion homeostasis. Neuroscience 129:877–896

Sykova E, Mazel T, Simonova Z (1998) Diffusion constraints and neuron–glia interaction during aging. Exp Gerontol 33:837–851

Takeda A, Sakurada N, Kanno S, Ando M, Oku N (2008) Vulnerability to seizure induced by dyshomeostasis in the hippocampus in aged rats. J Heal Sci 54:37–42

Takumi Y, Nagelhus EA, Eidet J, Matsubara A, Usami S, Shinkawa H, Nielsen S, Ottersen OP (1998) Select types of supporting cell in the inner ear express aquaporin-4 water channel protein. Eur J Neurosci 10:3584–3595

Venero JL, Vizuete ML, Machado A, Cano J (2001) Aquaporins in the central nervous system. Prog Neurobiol 63:321–336

Wen H, Nagelhus EA, Amiry-Moghaddam M, Agre P, Ottersen OP, Nielsen S (1999) Ontogeny of water transport in rat brain: postnatal expression of the aquaporin-4 water channel. Eur J Neurosci 11:935–945

Yasuda T, Bartlett PF, Adams DJ (2008) Kir and Kv channels regulate electrical properties and proliferation of adult neural precursor cells. Mol Cell Neurosci 37:284–297